Journal of Theoretical Physics

Founded and Edited by M. Apostol **197** (2010)

ISSN 1453-4428

Magic Binary Metallic Clusters

Liviu-Cristian Cune
Department of Theoretical Physics, National Institute for Physics and Nuclear Engineering, PO Box MG-6, RO-077125 Magurele-Bucharest, Romania
email: cune@theory.nipne.ro

Abstract

Structures and binding energies for bimetallic clusters consisting of a large variety of atomic species are obtained for all atomic sizes $N \leq 40$ and all concentrations, using an interatomic potential derived within a quasi-classical description. We find that increasing the difference between the two types of atoms leads to a gradual disappearance of the well-known homo-atomic geometric magic numbers and the appearance of magic pairs corresponding to the number of atoms of each atomic species in binary nanostructures with higher stability. This change is accompanied by structural transitions and ground-state↔isomer inversions, induced by changes in composition or concentration.

Experimental and theoretical results show that alloying atomic clusters can lead to new nano-materials with new properties and new functionalities. [1] Therefore, there is a need of detailed studies of such binary clusters, covering a wide range of atomic species. Since the computational effort limits the use of the ab-initio methods to selected compounds, guessed structures or imposed symmetries, so far such extensive studies have been performed using semi-empirical potentials, usually Lennard-Jones potentials (see for example Ref.[2]). Studies using semi-empirical potentials specific to metals, like second-moment approximation to tight-binding potentials, including Gupta [3] and Sutton-Chen [4] potentials, are focused on specific cluster sizes and compositions, occasionally for various concentrations. (See for example Refs. [5, 6, 7, 8]). Sometimes, the structures obtained with these semi-empirical potentials are locally re-optimized using density functional theory (DFT) methods. [5, 6]

We present here a more general approach, similar in some respect to the one presented in Ref. [2] for binary Lennard-Jones clusters. Using a genuine metallic potential derived and applied previously to homo-atomic clusters, [9] we search for the ground state structures for all binary clusters of size less than 40 and for any concentration; moreover, by varying the coupling constants in a range which covers a large number of metallic elements we try to map out the behavior of the bimetallic clusters in the compositional space. The theory employed in deriving these potentials has been applied also to homo-atomic clusters deposited on surfaces, [10] or to the metallic core of an iron-hydrocarbon cluster.[11] We could add also that the theory provides valuable information when applied to macroscopic object like metallic surfaces, infinite plates or slabs. It provides, for example, a theoretical derivation for the well known Smoluchowski ansatz [12] for the electron density at a metallic surface. [10] The theory applies straightforwardly to hetero-metallic compounds, the simplest case of free binary clusters being reported here.

Using a quasi-classical description for the electrons participating in a metallic bonding, it has been shown that the atomic interactions in a nanostructure can be described by an effective potential[9]

$$\Phi_{ij} = -\frac{1}{2} q z_i^* z_j^* \left(1 - \frac{2}{qR_{ij}}\right) e^{-qR_{ij}} \quad , \tag{1}$$

where R_{ij} are the interatomic distances, q is a variational screening wavevector and z_i^* are the effective ionic charges which depends on the atomic species.[1] It is worth mentioning here that long time ago a similar potential has been suggested on semi-empirical grounds, with some success, for the H_2 molecule. [13] These effective charges which play the role of coupling constants in the effective atomic interaction (1) can be estimated within the atomic screening theory. We have, for instance, $z_{Na}^* = 0.443$ for sodium, $z_{Ba}^* = 0.339$ for barium and $z_{Fe}^* = 0.579$ for iron. The equilibrium structures are obtained by minimizing the total potential energy, $\sum_{i<j} \Phi_{ij}$, and depend on q only as a scale factor for the atomic positions. For binary clusters, the equilibrium structures depends also on the ratio between the effective charges of the two atomic types. On the other hand, the binding energy depends on the values of both effective valence charges; it is obtained by minimizing the quasi-classical energy [9]

$$E_q = \frac{27\pi^2}{640} q^4 \sum_{i=1}^{N} z_i^* - \frac{3}{4} q \sum_{i=1}^{N} z_i^{*2} + \frac{1}{2} \sum_{i \neq j=1}^{N} \Phi_{ij} \quad , \tag{2}$$

[1] Atomic units are used: the Bohr radius $a_H \cong 0.53$Å for distances and $e^2/a_H \cong 27.2$eV for energies; $-e$ is the electron charge.

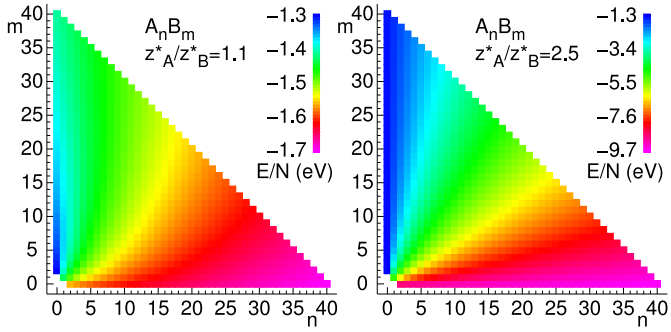

Figure 1: Binding energy per atom for binary clusters A_nB_m with $z_B^* = 0.3$.

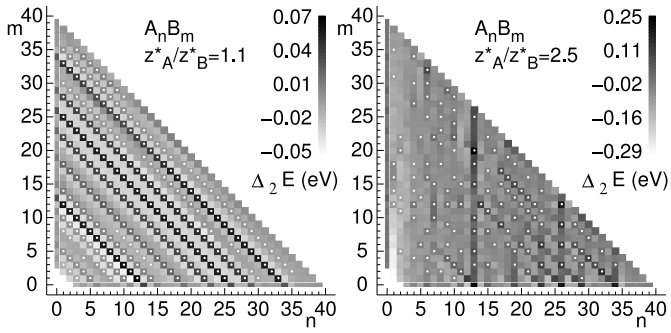

Figure 2: Stability spectrum for clusters A_nB_m.

with respect to the variational screening wavevector q, and by adding the exchange energy $E_{ex} = -(9/32)q^2 \sum_i z_i^*$. In equation (2) the first term is the kinetic energy of the electrons moving in the self-consistent Hartree field $\varphi = \sum_i z_i^* \exp(-q\,|\mathbf{r} - \mathbf{R}_i|)/\,|\mathbf{r} - \mathbf{R}_i|$, where $\mathbf{R}_i$ are the atomic positions, and having the electron density $n = q^2\varphi/4\pi$; the second term plays the role of an electron self-energy and the last term is the total potential energy.

It is worth emphasizing that the effective potential given by equation (1) is a genuine many-body potential because the variational screening wavevector q has an implicit dependence on all the atomic positions $\mathbf{R}_i$. On the other hand, in the numerical problem of finding equilibrium cluster structures we can avoid the difficult task of minimizing an energy composed of multiparticle potentials by minimizing first a reduced total potential energy, E_{pot}/q, with respect to the scaled positions $q\mathbf{R}_i$.

The theory outlined above has been applied to binary clusters A_nB_{N-n}, with $N = \overline{2,40}$, $n = \overline{0,N}$ and the ratio $1 \leq z_A^*/z_B^* \leq 2.5$ (step 0.1) of the effective valence charges of the two elements A and B. These parameters cover a very large domain of binary metallic compounds. The minimization of the potential energy has been performed by usual gradient method starting from random initial positions. The use of large statistical ensembles is required by the increasing number of isomers compared with the homo-atomic case; each isomer is accompanied by the so called homotops, clusters which, up to permutations between different type of atoms, share approximately the same geometric structure and energy. A way to overcome this difficulty is to make such permutations during the minimization of the potential energy, provided they are energetically favorable. Because other authors use the word composition with other meaning it is important to specify that we use the term concentration for the ratio between the number of atoms A and the total number of atoms and composition for the ratio z_A^*/z_B^*. With this conventions, a changed concentration means that some atoms A are replaced by atoms of type B (or vice versa) and a changed compositions means that all the atoms of one type (say A for example) are replaced by atoms of another type (say C for example) and this change is reflected in a variation of the ratio z_A^*/z_B^*. The ground-state binding energies per atom for two values of the ratio z_A^*/z_B^* are presented in Figure 1. The energies presented in Figure 1 correspond to $z_B^* = 0.3$ but can be easily scaled to different values of z_B^*. We can see in Figure 1 how the energy range increases for higher z_A^*/z_B^* values; we obtain, for instance, a range of less than 0.5eV for $z_A^*/z_B^* = 1.1$ and more than 8eV for $z_A^*/z_B^* = 2.5$. This energy range variation can be understand as a rapid change in the mean effective valence charge when we change the concentration for clusters composed of very dissimilar atoms.

For homo-atomic clusters the stability with respect to the variation of the number of atoms is tested by the second difference of the energy; [14] it defines the so called stability spectrum, sometimes well correlated with the experimental mass-abundance spectrum; its maxima indicate the magic numbers, clusters with higher stability compared to their neighbors. The magic numbers obtained for homo-atomic metallic clusters are 6, 13, 19, 23, 26, 29, 34, ... ;[9] these numbers, now known as geometrical magic numbers, because they are given by the close

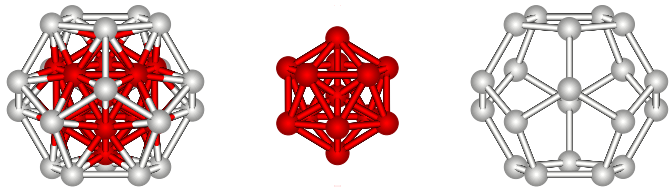

Figure 3: The cluster $A_{13}B_{20}$ (*left*), magic for $z_A^*/z_B^* \geq 1.7$ and ground-state for $z_A^*/z_B^* \geq 1.6$, displaying an A_{13} icosahedron core (*center*) and a B_{20} dodecahedron shell (*right*).

packing in the icosahedral structures, have been obtained with various other methods like, for example with Morse potentials. [15] For binary clusters we can define two families of such spectra for each type of atoms:

$$\begin{aligned} \Delta_2^A E &= E_{n+1,m} + E_{n-1,m} - 2E_{n,m} \\ \Delta_2^B E &= E_{n,m+1} + E_{n,m-1} - 2E_{n,m} \end{aligned} \tag{3}$$

where $E_{n,m}$ is the binding energy of the binary cluster A_nB_m, $\Delta_2^A E$ and $\Delta_2^B E$ indicate the cluster stability with respect to the variation of the number of A-atoms (or B-atoms respectively) at fixed number of B-atoms (or A-atoms respectively). Each spectrum has magic numbers; the coincidence of a maximum in both spectra define a magic pair $\{n, m\}$, *i.e.* a double magic clusters A_nB_m. The maxima in a sum spectrum defined as $\Delta_2 E = \Delta_2^A E + \Delta_2^B E$ can also be viewed as magic pairs; by analogy with the homo-atomic case,[9] we can define a relative abundance $D = \ln I_{n,m}^4 / I_{n+1,m} I_{n-1,m} I_{n,m+1} I_{n,m-1}$, where $I_{n,m}$ is the Boltzmann statistical weight; up to a constant we have $D \simeq \Delta_2 E$. We have found a very close similarity between the results obtained with these two definitions in the whole range of effective valence charges we have studied. The definitions given here for magic pairs follows closely the definition for magic numbers in homo-atomic clusters, which reflects an enhanced stability relative to all the neighbors with one atom more or one atom less. The definition of magic spectra reflect also the condensation and evaporation processes that take place in a majority of experimental setups. Only the first order processes (involving loosing or acquiring of a single atom) are taken into account. It is somehow tempting to consider also, for example, the cluster $A_{n-1}B_{m+1}$ as a neighbor of A_nB_m in the stability spectrum; but A_nB_m can evolve into $A_{n-1}B_{m+1}$ or vice versa only through second order processes (losing an atom of one type and acquiring an atom of another type). Stability relative to such neighbors can be tested by defining a spectrum at fixed size and variable concentration. [1, 7, 16]

The sum spectrum defined above is shown in Figure 2 for two values of z_A^*/z_B^*; the darker squares indicate magic pairs; also, the magic pairs according to the first definition are marked with white dots; we can see the above mentioned similarity between the two definitions. We can see in Figure 2 that for small values of the ratio z_A^*/z_B^* the magic pairs correspond to the homo-atomic magic numbers for $N = n + m$. Once the discrepancy between atomic species increases, this homo-atomic behavior gradually disappears giving place to new magic pairs. This can be explained by the small distortions in the icosahedral symmetry caused by the small difference in the interatomic interactions $A - A$, $A - B$, $B - B$, and by structural transitions to fcc or disordered geometries. The magic pairs are confined to certain regions in the range of the parameter z_A^*/z_B^*. Varying the composition, the magic peaks gradually appear, starting with some value z_A^*/z_B^* and may vanish at a higher z_A^*/z_B^* value. We obtained, for instance, the magic pairs {6,32} for $z_A^*/z_B^* \geq 1.4$, {10,22} for $1.5 \leq z_A^*/z_B^* \leq 2.4$, {13,20} for $z_A^*/z_B^* \geq 1.7$, {14,24} for $1.4 \leq z_A^*/z_B^* \leq 2.0$ and {26,12} for $z_A^*/z_B^* \geq 1.8$, which correspond to clusters having N=32, 33 or 38 which are not homo-atomic magic numbers.[9]

In the lowest range of the z_A^*/z_B^* values the equilibrium structures have with preponderance icosahedral symmetry and display a core-shell atomic arrangement, with the 'heavier', *i.e.* greater effective charge, A-atoms in the center and a B-atoms shell. There is experimental and theoretical evidence for this radial segregation in binary clusters (see for example Refs. [5, 17, 18]). In our model segregation is favored over mixing because the strength of the $A - B$ interaction is always smaller than the $A - A$ interaction. The A atoms segregate in the center where atoms have greater coordination numbers and an increasing number of $A - A$ bonds is energetically favorable. The mixing could take place if $A - B$ had been the strongest interaction. [1] Although new structures and symmetries appear, the icosahedral symmetry is often obtained for larger values of the ratio of the effective charges of the two atomic species. For example, the magic cluster $A_{13}B_{20}$, whose structure is presented in Figure 3, has a perfect icosahedral symmetry and a core-shell atomic arrangement with a core icosahedron formed by the A-atoms and an outside shell of B-atoms grouped in a perfect dodecahedron. The high stability of this cluster can be explained by the favorable ratio of the numbers of atoms A and B (favorable concentration). The A_{13}-icosahedron core is also magic in the homo-atomic series. In spite of different strengths in the inter-atomic interaction, each atom species occupies distinct icosahedral shells, which do not lead to symmetry distortions, and gives stability. Moreover, the

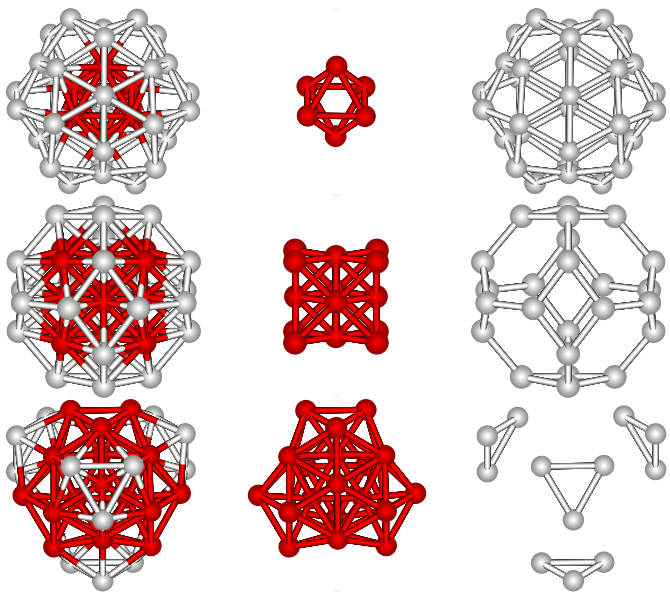

Figure 4: The bimetallic 38-atoms cluster corresponding to the magic pairs {6,32} (the top row), {14,24} (the middle row) and {26,12} (the bottom row).

strength of the inter-atomic interaction $A-B$, greater than the $B-B$ interaction, equilibrates the incomplete outside shell (the so called anti-Mackay shell which becomes complete at $N=45$) by maximizing the numbers of $A-B$ bounds in detriment of the weaker $B-B$ bounds. Once the ratio between the two effective charges is decreased this geometric arrangement becomes energetically unfavorable, the homo-atomic ground-state having a rather disordered structure. This is a first example of structural transition induced by composition. Such core-magic structures (the core is magic itself, as a homo-atomic cluster) which are also stable against the variation of the number of B atoms, forming in this way magic pairs, have been obtained, usually for higher z_A^*/z_B^* values, for various magic numbers of A-atoms. For instance, we can identify the magic pairs $\{6,32\}$, $\{13,20\}$, $\{23,m\}$, whit $m=3$, 6 and $\{26,m\}$, with $m=3$, 6, 9, 12. A particular cluster is the 38-atoms clusters which becomes highly stable, in different equilibrium structures, for the magic pairs $\{6,32\}$, $\{14,24\}$ and $\{26,12\}$. The equilibrium geometric forms for these clusters are shown in Figure 4. The clusters A_6B_{32} and $A_{26}B_{12}$ belong to the above mentioned core-magic structures. The structure $A_{14}B_{24}$ has a fcc symmetry, his A_{14}-core being a face centered cube and the outside B_{24}-shell a truncated octahedron.

The structures presented in Figure 4 suggest an icosahedral-fcc transition for the A_nB_{38-n} clusters driven by the variation of concentration (variation of n) at fixed composition (at fixed z_A^*/z_B^* ratio). A similar transition, has been previously reported for the binary clusters Co_mPt_{38-m}, [7] for the 38-atoms mixed rare-gas clusters [19] and Morse binary clusters. [16] This type of transition has been obtained for various cluster sizes, especially at large z_A^*/z_B^* ratio.

A new kind of structural transition, a composition induced transition, is obtained for fixed numbers of atoms A and B (fixed concentration), by varying z_A^*/z_B^*, *i.e.* by replacing at least one type of atom with one having a different effective charge. For instance, the cluster $A_{14}B_{24}$ has two structural transitions, its ground-state being of icosahedral type (slightly disordered) for $z_A^*/z_B^* \leq 1.2$, fcc for $1.3 \leq z_A^*/z_B^* \leq 2.2$ and icosahedral for $z_A^*/z_B^* \geq 2.3$. The existence of these structural domains bounded by structural transition points is a general feature of binary clusters. Because we have performed our study with step 0.1 of the parameter z_A^*/z_B^* we can identify with this accuracy the location of the transition points. For instance, in the above example, we have two transition points, one located between $1.2-1.3$ and another between $2.2-2.3$. Often, for the left-right values which border the transition points we can observe ground-state$\longleftrightarrow$isomer inversions, *i.e.* the left ground-state becomes the right isomer and (or) the left isomer becomes the right ground-state. This implies that, at the transition points, the ground state is degenerate; we have two structures with different symmetries but with the same cohesion energy. Of course, there remains the question of finding two atomic species whose effective valence ratio has this critical value. On the other hand, even if we find such atomic species, it is likely that quantum corrections to the quasi-classical description[9] remove this degeneracy. In this respect, the correct conclusion is that it is possibly to synthesize binary metallic clusters, made up of specific atoms, with very small gaps between the ground-state and the first isomers. These small gaps could imply an increased experimental abundance even if they are not magic (the theoretical abundance spectrum is referred to the ground-state structures; the existence of such small gaps for specific compositions could locally alter this spectrum). On the other hand the task of producing clusters with a

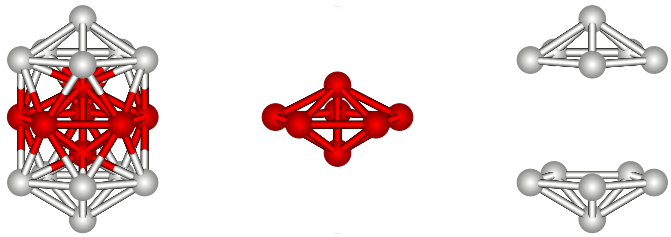

Figure 5: (Color online) The domain walls segregation in the cluster A_7B_{12} irrespective of the ratio z_A^*/z_B^*.

specific geometry will become difficult in the presence of this shape degeneracy.

Beside the core-shell segregation, which is dominant for binary nano-clusters, we can identify another type of segregation. In some structures the B-atoms occupy two distinct regions (up-down) separated by an A-atoms region. This kind of domains walls segregation is very rare, the core-shell segregation being predominant; it has been obtained for the cluster A_7B_{12}, whose structure is presented in Figure 5. A similar segregation has been obtained for the Lennard-Jones cluster A_7B_{12} [2] and also in $Co-Pd$ nanoclusters for sizes $N = 13$ and $N = 19$, using a genetic algorithm in combination with a Gupta potential. On the other hand the segregation shown in Figure 5 can be described as a surface segregation, because the 12 B atoms, instead of forming a uniform closed surface around the 7 atoms A-core, segregate in two distinct regions diametrically opposite on that surface. Moreover, a surface segregation can be observed also in the structure of the cluster $A_{26}B_{12}$ shown in Figure 4. There, the 12 B atoms forming the outside shell segregate in 4 distinct regions, each region consisting of 3 B atoms closely bound together. Such a surface segregation could be interpreted as a variable surface composition in experimental measurements. Evidence for a variable surface composition in Ar/Xe clusters in photoelectron spectroscopy has been reported in Ref. [17].

In conclusion, we have obtained the general characteristics of binary metallic clusters: the magic pairs in the stability spectra, the radial, domain walls and surface segregation and the structural transitions induced by change in composition or concentration. These features are expected to hold also for larger binary clusters although new structures and segregation types could appear. It is worth noting that by adding an interaction energy with a metallic surface[10] to the quasi-classical energy given by (2), the present approach can be applied to binary metallic clusters deposited on surfaces, which is the common environment for most of the intended technical applications.

The author is indebted to M. Apostol for useful discussions. This work was partially supported by Contract Nos CEx05-D11-67 and PN-09-37-01-02 of the Romanian Ministry of Education and Research.

References

[1] R. Ferrando, J. Jellinek and R. Johnston, Chem. Rev. **108**, 845 (2008).

[2] J. P. K. Doye and L. Meyer, Phys. Rev. Lett. **95**, 063401 (2005); arXiv:cond-mat/0604250v1.

[3] R. P. Gupta, Phys. Rev. B **23**, 6265 (1981); V. Rosato, M. Guillope and B. Legrand, Philos. Mag. A **59**, 321 (1989).

[4] A. P. Sutton and J. Chen, Philos. Mag. Lett. **61**, 139 (1990).

[5] G. Rossi *et al.*, Phys. Rev. Lett. **93**, 105503 (2004).

[6] G. Barcaro *et al.*, J. Phys. Chem. B **110**, 23197 (2006).

[7] Q. L. Lu *et al.*, Phys. Lett. A **350**, 258 (2006).

[8] C. Massen, T. V. Mortimer-Jones and R. L. Johnston, J. Chem. Soc., Dalton Trans., 4375 (2002); L. D. Lloyd *et al.*, J. Mater. Chem. **14**, 1691 (2004); F. Aguilera-Granja *et al.*, Phys. Rev. B 74, 224405 (2006).

[9] L. C. Cune and M. Apostol, Phys. Lett. A **273**, 117 (2000).

[10] L. C. Cune and M. Apostol, in *Low-Dimensional Systems: Theory, Preparation, and Some Applications*, 1, eds. Luis M. Liz-Marzan et al. (Kluwer Academic Publisher, 2003); Dig. J. Nano. Bio. **2**, 315 (2007).

[11] L. C. Cune and M. Apostol, Chem. Phys. Lett. 344, 287 (2001).

[12] R. Smoluchowski, Phys. Rev. **60** 661 (1941).

[13] A. A. Frost and B. Muslin, J. Chem. Phys. **22** 1077 (1954).

[14] W. A. de Heer, Rev. Mod. Phys. **65**, 611 (1993); M. Brack, Rev. Mod. Phys. **65**, 677 (1993); F. Baletto and R. Ferrando, Rev. Mod. Phys. **77**, 371 (2005).

[15] J. P. K. Doye and D. J. Wales. J. Chem. Soc. Faraday Trans. **93**, 4233 (1993).

[16] D. Parodi and R. Ferrando, Phys. Lett. A **367**, 215 (2007).

[17] M. Tchaplyguine *et al.*, Phys. Rev. A **69**, 031201R (2004).

[18] F. Calvo, E. Cottancin and M. Broyer, Phys. Rev. B **77**, 121406R (2008); M. Cazayous *et al.*, Phys. Rev. B **73**, 113402 (2006); M. Gaudry *et al.*, Phys. Rev. B **67**, 155409 (2003).

[19] F. Calvo and E. Yurtsever, Phys. Rev. B **70**, 045423 (2004).